JOC Article

Synthesis of Bispyrenyl Sugar-Aza-Crown Ethers as New Fluorescent Molecular Sensors for Cu(II)

Juan Xie,*,† Mickaël Ménand,‡ Stéphane Maisonneuve,† and Rémi Métivier*,†

PPSM, Institut d'Alembert, ENS Cachan, CNRS, UniverSud, 61 Avenue du President Wilson, F-94230 Cachan, France, and Synthèse, Structure et Fonction des Molécules Bioactives, CNRS UMR 8531, Université Pierre et Marie Curie, 4 place Jussieu, F-75005 Paris, France

joanne.xie@ppsm.ens-cachan.fr; metivier@ppsm.ens-cachan.fr

Received February 15, 2007

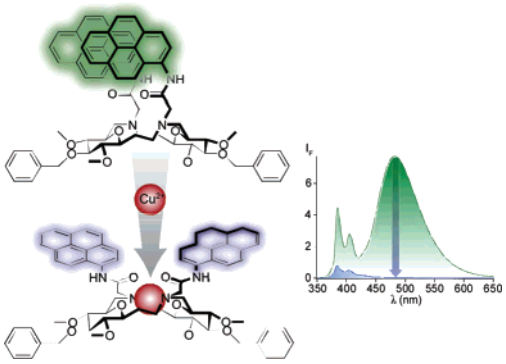

Two *N*-pyrenylacetamide-substituted sugar-aza-crown ethers have been synthesized as new fluorescent chemosensors. The designed ligands **1** and **2** exhibit fluorescence characteristics of a pyrene monomer and a dynamic excimer emission when compared to *N*-pyrenylacetamide as a model compound. Both ligands displayed a Cu^{2+}-sensitive fluorescence quenching with a 1:1 stoichiometry and high stability constants (log $K = 6.7$ for **1** and 7.8 for **2**). The quenching effect was rationalized on the basis of photoinduced electron transfer from the excited pyrene to the complexed Cu^{2+} cation, while the changes in excimer-to-monomer ratio were explained by a conformational analysis through DFT calculations. The predicted structure suggests that the Cu^{2+} cation is coordinated with the two carbonyl groups and the sugar-aza-crown ethers which rigidified the complex structure and placed the two pyrene moieties far apart.

Introduction

Much recent effort has been devoted to the design and synthesis of new fluorescent chemosensors that can be used for the sensing and recognition of environmentally and biologically important ionic species.[1] Typically, fluorescent chemosensors for ions, also called fluoroionophores, consist of an ion recognition unit (ionophore) and a fluorogenic unit (fluorophore) linked together through a proper spacer. As fluorogenic groups, pyrenyl substituents are very attractive because of their efficient monomer and excimer emission. Using fluorescence changes in intramolecular excimer emission or fluorescence quenching, various pyrene-based ligands (e.g., lariat ether,[2] calix[4]arenes,[3] calix-aza-crown,[4] cyclam,[5] diazatetrathia-crown ether,[6] pentiptycene,[7] or hinge sugar[8]) have been developed as fluorophores

† UniverSud.

‡ Université Pierre et Marie Curie.

(1) Selected books and reviews: (a) Valeur, B.; Leray, I. *Coord. Chem. Rev.* **2000**, *205*, 3−40. (b) Desvergne, J. P., Czarnik, A. W., Eds. *Chemosensors of Ion and Molecule Recognition;* Kluwer Academic Publishers: Dordrecht, The Netherlands, 1997. (c) de Silva, A. P.; Gunaratne, H. Q. N.; Gunnlaugsson, T.; Huxley, A. J. M.; McCoy, C. P.; Rademacher, J. T.; Rice, T. E. *Chem. Rev.* **1997**, *97*, 1515−1566. (d) Callan, J. F.; de Silva, A. P.; Magri, D. C. *Tetrahedron* **2005**, *61*, 8551−8588.

(2) Nakahara, Y.; Toshiyuki, K.; Nakatsuji, Y.; Akashi, M. *J. Org. Chem.* **2004**, *69*, 4403−4411.

(3) (a) Kim, J. S.; Lee, S. H.; Lee, J. Y.; Bartsch, R. A.; Kim, J. S. *J. Am. Chem. Soc.* **2004**, *126*, 16499−16506. (b) Lee, S. H.; Kim, S. H.; Kim, S. K.; Jung, J. H.; Kim, J. S. *J. Org. Chem.* **2005**, *70*, 9288−9295. (c) Kim, S. H.; Choi, J. K.; Kim, S. K.; Sim, W.; Kim, J. S. *Tetrahedron Lett.* **2006**, *47*, 3737−3741. (d) Jin, T.; Ichikawa, K.; Koyama, T. *J. Chem. Soc., Chem. Commun.* **1992**, 499−501.

(4) Kim, J. H.; Hwang, A.-H.; Chang, S.-K. *Tetrahedron Lett.* **2004**, *45*, 7557−7561.

(5) Moon, S.-Y.; Youn, N. J.; Park, S. M.; Chang, S.-K. *J. Org. Chem.* **2005**, *70*, 2394−2397.

10.1021/jo070315y CCC: $37.00
Published on Web 07/12/2007

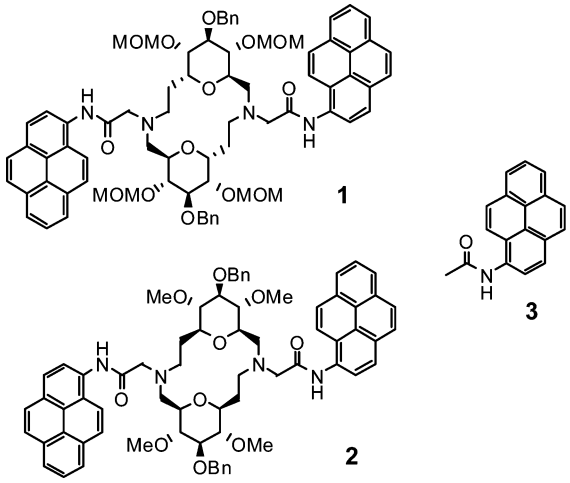

FIGURE 1. Structures of pyrenyl SACs **1** and **2** and *N*-pyrenylacetamide **3**.

to the selective detection of transition or heavy metal ions, in particular Hg^{2+}, Cu^{2+}, and Zn^{2+} ions. We have recently developed the synthesis of sugar-aza-crowns (SACs) as new sugar-based molecular receptors.[9] SACs with appropriate appended chromophores would be good candidates for cation probes because of their aza-crown structures which can be used as a cation recognition unit.[9c] We then decided to introduce two pyrenylacetamide groups into the two nearby placed nitrogen atoms of SACs that might act as a sensitive probe by exhibiting changes in either monomer or excimer emissions, depending on the state of the ionophore upon the interaction with targeting metal ions or the relative proximity of the two pyrene moieties. For this study, two configurational different ligands **1** (α-gluco) and **2** (*β*-gluco) have been prepared (Figure 1). Both ligands exhibit a Cu^{2+}-sensitive fluorescence quenching with a concomitant change in excimer-to-monomer ratio, and we rationalized this fluorescence behavior on the basis of ab initio calculations.

Results and Discussion

Compounds **1** and **2** can be easily prepared from SACs by a one-step reaction. Treatment of SAC **4**[9b] or **6**[9b] with *N*-(1-pyrenyl)chloroacetamide **5**[4] using K_2CO_3 as a base in CH_3CN in the presence of KI and nBu$_4$NI[10] at reflux gave the expected compounds **1** and **2** in 80 and 29% yield, respectively (Scheme 1). The lower yield of **2** can be explained by a loss of product during HPLC purification.

The chemosensor behavior was investigated by the fluorescence measurement in MeOH solution (2 μM) upon excitation at 340 nm. As shown in Figure 2, ligands **1** and **2** display fluorescence characteristics of pyrene monomer (λ_{max} = 385 nm) and excimer emission ($\lambda_{max} \approx$ 480 nm). Very similar absorption spectra and molar absorption coefficients were found for the two ligands: $\epsilon_{385nm} = 5.0 \pm 0.1 \times 10^4$ L mol^{-1} cm^{-1} for **1** and $5.4 \pm 0.1 \times 10^4$ L mol^{-1} cm^{-1} for **2**. Since **1** and **2** contain two pyrenyl substituents, this is consistent with the value obtained for the PyAc (*N*-pyrenylacetamide) **3**[11] model chromophore ($\epsilon_{385nm} = 2.7 \pm 0.1 \times 10^4$ L mol^{-1} cm^{-1}). Only a slight broadening of the absorption vibrational features was observed between the ligands and PyAc. Moreover, very limited red shifts (below 3 nm for both ligands) of the fluorescence excitation spectra at excimer emission (λ_{em} = 485 nm) compared to the ones at monomer emission (λ_{em} = 405 nm) were observed (see spectra in Supporting Information). As a conclusion, preformed dimer species at the ground state, although not negligible, were estimated to be very low. Interestingly, the fluorescence behavior of both ligands is dependent on the relative configuration of SACs, with excimer emission of **1** weaker than that of **2**: the relative integrated intensity of the excimer and monomer emission bands (I_{Exc}/I_{Mon}) was found to be 1.3 for **1** and 5.4 for **2**. This is probably due to different conformations adopted by these two diastereomeric ligands. However, the relative intensity of the excimer and monomer emission bands was found to be independent of ligand concentration in the range of 2×10^{-7} mol L^{-1} up to 10^{-5} mol L^{-1}, which is consistent with formation of an intramolecular excimer due to strong $\pi-\pi$ interaction between two pyrenyl units. The fluorescence quantum yields of the monomer contributions were then measured to be 0.073 and 0.035 for ligands **1** and **2**, respectively. The monomer fluorescence quantum yields of ligands **1** and **2** are lower than the value obtained for the model compound PyAc (Φ_F = 0.080). This effect is well-correlated to the strong excimer emission observed for the two sugar-aza-crown ligands.

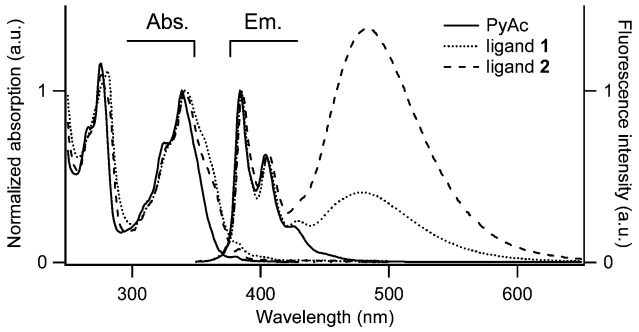

FIGURE 2. Normalized absorption and emission spectra of the model compound PyAc ($c = 4 \times 10^{-6}$ mol L^{-1}) and ligands **1** and **2** ($c = 2 \times 10^{-6}$ mol L^{-1}) in MeOH. λ_{ex} = 340 nm.

The proportion of excimer emission showed a sensitive dependence on the polarity of the solvent, being much less important in the less polar solvents such as CH_2Cl_2 and THF (Figure 3). It is actually well-known that interactions of pyrene with the solvent are favored in nonpolar media.[12,13] Stabilized monomer conformations with separated pyrene chromophores induce therefore a larger monomer contribution to the fluorescence emission in such solvents. Conversely, excimer formation is favored in polar solvents, leading to a greater intensity of

(6) Kim, S. H.; Song, K. C.; Ahn, S.; Kang, Y. S.; Chang, S.-K. *Tetrahedron Lett.* **2006**, *47*, 497−500.

(7) Yang, J.-S.; Lin, C.-S.; Hwang, C.-Y. *Org. Lett.* **2001**, *3*, 889−891.

(8) (a) Yuasa, H.; Miyagawa, N.; Izumi, T.; Nakatani, M.; Izumi, M.; Hashimoto, H. *Org. Lett.* **2004**, *6*, 1489−1492. (b) Yuasa, H.; Miyagawa, N.; Nakatani, M.; Izumi, M.; Hashimoto, H. *Org. Biomol. Chem.* **2004**, *2*, 3548−3556.

(9) (a) Ménand, M.; Blais, J. C.; Hamon, L.; Valéry, J. M.; Xie, J. *J. Org. Chem.* **2005**, *70*, 4423−4430. (b) Ménand, M.; Blais, J. C.; Valéry, J. M.; Xie, J. *J. Org. Chem.* **2006**, *71*, 3295−3298. (c) Fournier, F.; Afonso, C.; Ménand, M.; Hamon, L.; Xie, J.; Tabet, J.-C. Proceeding of the 54th ASMS Conference on Mass Spectrometry and Allied Topics, Seattle, WA, May 28−June 1, 2006; ASMS: Santa Fe, NM, 2006.

(10) Calvet, S.; David, O.; Vanucci-Bacqué, C.; Fargeau-Bellasoued, M.-C.; Lohmmet, G. *Tetrahedron* **2003**, *59*, 6333−6339.

(11) Kerr, C. E.; Mitchell, C. D.; Headrick, J.; Eaton, B. E.; Netzel, T. L. *J. Phys. Chem. B* **2000**, *104*, 1637−1650.

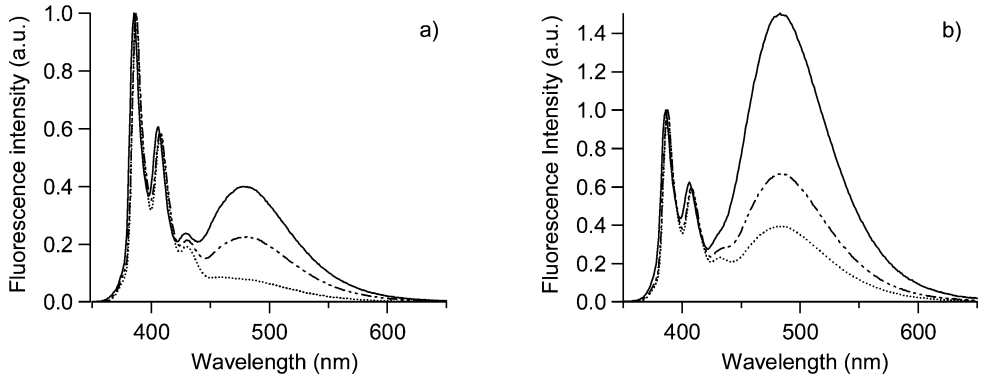

FIGURE 3. Monomer-normalized fluorescence spectra of ligands **1** (a) and **2** (b) in different solvents: MeOH (—), CH_2Cl_2 (— · —), and THF (···). $\lambda_{ex} = 340$ nm.

SCHEME 1. Synthesis of Pyrenyl SACs 1 and 2

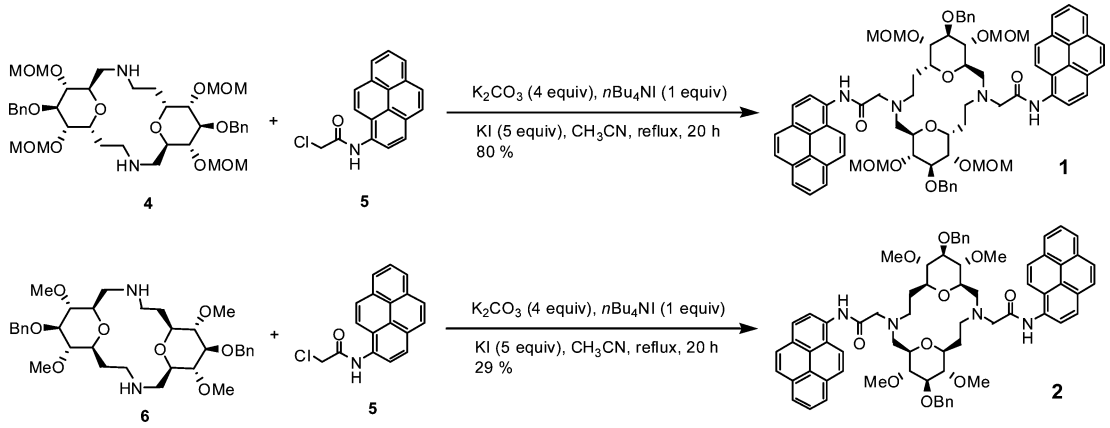

excimer emission.[5,12] On the basis of these observations, we decided to investigate metal complexation properties in MeOH solution.

Since both ligands have basic amino groups in the molecular framework that might influence the fluorescence behavior of the ionophore, we tried to evaluate the influence of pH on the fluorescence properties. No influence was observed on the fluorescence emission spectra of **1** and **2** in the presence of a large excess of acetic acid or triethylamine (2000 equiv) (see spectra in Supporting Information). To get insight into the binding properties of both ligands toward metal ions, we first investigated fluorescence changes upon addition of 100 equiv of perchlorate salts of divalent cations to the MeOH solution of **1** or **2**. As presented in Figure 4, the total fluorescence intensity was not significantly affected by a representative selection of alkaline earth metal ions (Mg^{2+}, Ca^{2+}) and transition-metal ions (Co^{2+}, Mn^{2+}, Ni^{2+}). The fluorescence emission was strongly quenched by Cu^{2+} with a 97.5% efficiency. Interestingly, a quenching effect was also observed for Cd^{2+} (90% efficiency with ligand **2**, but no effect by adding only 1 equiv of cation) and to a less extent for Pb^{2+} and Zn^{2+} (with ligand **1**). A similar quenching effect induced by Pb^{2+} and Zn^{2+} ions has also been observed with *N*-pyrenylacetamide-substituted calix[4]arenes derivatives.[3] Nevertheless, the selectivity toward Cu^{2+} was further ascertained by the competition experiment by adding 100 equiv of Cu^{2+} ions to the competing metal ion−ligand mixtures, where the emission was quenched as in the presence of Cu^{2+} alone (Figure 4).

The binding process of Cu^{2+} ion to both ligands was found to be slow. Three hours were required to reach the equilibrium. This slow rate of binding probably reflects the steric hindrance of the two bulky pyrenylacetamide groups to the approach of the metal ions. Consequently, the titration solutions have been prepared the previous day. The complexation experiment was realized by both absorption and fluorescence measurements. As the concentration of Cu^{2+} increases, the fluorescence intensity is progressively quenched (Figures 5 and 6 for ligands **1** and **2**, respectively). The insets of Figures 5 and 6 show the decrease of fluorescence intensity as a function of Cu^{2+} concentration. The curves were well-fitted with a 1:1 complexation equation model and provided high stability constants as followed: log $K(Cu^{2+}$:**1**$) = 6.7 \pm 0.2$ and log $K(Cu^{2+}$:**2**$) = 7.8 \pm 0.3$. The complexation curves are linear until 1.0−1.5 μM (60−100 μg L^{-1}). Under these experimental conditions, the detection limit of Cu^{2+}, calculated as three times the standard deviation of the background noise from the calibration curve, was found to be 40 nM (2.5 μg L^{-1}) for both ligands. Furthermore, the decrease of the excimer-to-monomer ratio until the total disappearance of the excimer emission allows a ratiometric measurement. Figure 6b shows the decrease of the I_{Exc}/I_{Mon} ratio of ligand **2** while increasing the Cu^{2+} concentration. The shape of the curve was successfully fitted to the theoretical behavior with the binding constant determined previously (log $K(Cu^{2+}$:**2**$) = 7.8$

(12) Parker, D.; Williams, J. A. G. *J. Chem. Soc., Perkin Trans. 2* **1995**, 1305−1314.
(13) (a) Métivier, R.; Leray, I.; Lefèvre, J.-P.; Roy-Auberger, M.; Zanier-Szydlowski, N.; Valeur, B. *Phys. Chem. Chem. Phys.* **2003**, *5*, 758−766. (b) Lochmüller, C. H.; Kersey, M. T. *Anal. Chim. Acta* **1987**, *200*, 143.
(14) Rurack, K. *Spectrochim. Acta, Part A* **2001**, *57*, 2161−2195.

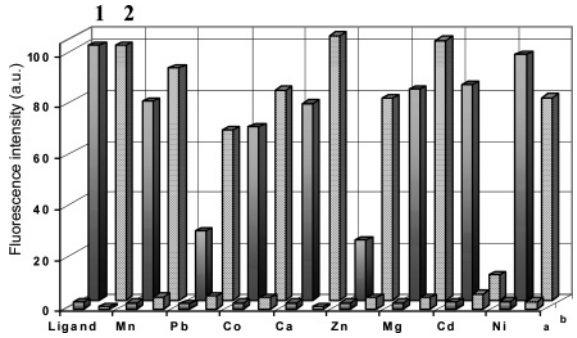

FIGURE 4. Fluorescence intensity change profiles of **1** and **2** (5×10^{-6} M) in MeOH with selected cations (5×10^{-4} M) in the absence (b) or presence (a) of Cu^{2+} (5×10^{-4} M). $\lambda_{ex} = 340$ nm.

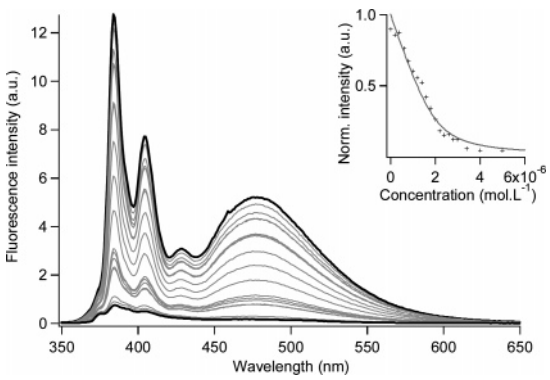

FIGURE 5. Fluorescence spectra obtained during the titration of **1** in MeOH ($c = 2 \times 10^{-6}$ M) with $Cu(ClO_4)_2$ (from 0 to 2.5 equiv). $\lambda_{ex} =$ 340 nm. Inset: titration curve of the normalized integrated fluorescence as a function of Cu^{2+} concentration.

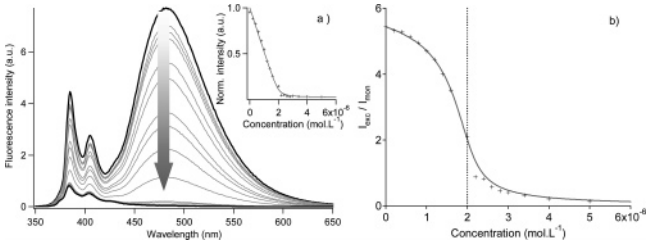

FIGURE 6. (a) Fluorescence spectra obtained during the titration of **2** in MeOH ($c = 2 \times 10^{-6}$ M) with $Cu(ClO_4)_2$ (from 0 to 2.5 equiv). $\lambda_{ex} = 340$ nm. Inset: titration curve of the normalized integrated fluorescence as a function of Cu^{2+} concentration. (b) Relative intensity of the excimer and monomer emission bands (I_{Exc}/I_{Mon}) as a function of Cu^{2+} concentration.

$\pm$ 0.3; Supporting Information). Such a ratiometric measurement is of great advantage because it is independent of the total concentration of ligand, the fluctuations of the source intensity and the sensitivity of the instrument.[1a] Thus, determination of Cu^{2+} in the range of 1 equiv, where the response change is maximized (around 2×10^{-6} M in the present experiment), can be achieved in a very reproducible and accurate way. The design of fluoroionophores for Cu^{2+} is still very attractive because this metal ion is not only an essential trace element in a biological system, but also a widely used metal pollutant.[14,15] Copper ion is also one of the major sources of oxidative stress that is closely related to neurogenerative diseases.[16] Very few carbohydrate-based Cu^{2+} ion fluorosensors have been reported.[17] The sugar-aza-crown-based ligands **1** and **2** have similar or higher binding constants compared to that of cyclam-derived

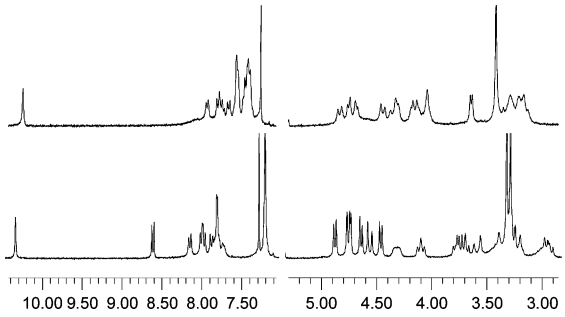

FIGURE 7. ^1H NMR spectra of ligand **1** in the absence (bottom) and presence (top) of 5.0 equiv of $Zn(ClO_4)_2$ (after 48 h equilibrium) in $CDCl_3$.

probes.[18] The complex formation of ligand **1** with Cu^{2+} was also evidenced by IR measurement: the carbonyl band was shifted from 1690 to 1618 cm^{-1} for **1**.

The remarkable fluorescence quenching induced by the Cu^{2+} cation can be tentatively ascribed by a photoinduced electron transfer (PET) from the excited pyrene fluorophore to the complexed Cu^{2+} cation.[14] Actually, the electrochemical potentials of the PyAc chromophore and the Cu^{2+} ion were measured: $E(PyAc^{\bullet+}/PyAc) = +0.75$ V (vs Fc^+/Fc in desaerated acetonitrile/toluene) and $E(Cu^{2+}/Cu^+) = -0.26$ V (vs Fc^+/Fc in desaerated MeOH). The energy of the pyrene excited state, as estimated from the average of the first absorption band and the emission band maxima, is around 3.4 eV. The photoinduced electron transfer is therefore thermodynamically allowed, and the free energy can be estimated to be around $\Delta G_{ET} = -2.4$ eV. In addition, the cation-induced decrease on excimer-to-monomer fluorescence ratio reveals strong conformational changes of the ligands caused by coordination with Cu^{2+}, which could reduce the conformational degrees of freedom of the two pyrenyl substituents and inhibit any intramolecular $\pi-\pi$ stacking of the pyrene groups.

Since Cu^{2+} is a paramagnetic ion, not very suitable for NMR experiments, we then decided to investigate the complexation of ligand **1** with Zn^{2+}. ^1H NMR showed that addition of $Zn(ClO_4)_2$ (5 equiv) to the $CDCl_3$ solution of **1** induced upfield shifts of the amide proton (from 10.36 to 10.25 ppm) and aromatic pyrene protons (in particular protons at 8.63 ppm) (Figure 7). Significant shifts and broadening have also been observed for the SAC protons (2.90−4.90 ppm). These results indicated a significant conformational change of the SAC ring as a consequence of Zn^{2+} complexation.

To investigate the possible metal ion binding sites in the ligands, we then performed density functional theory (DFT) calculations with Becke-3-Lee−Yang−Parr (B3LYP) exchange functionals using the Gaussian 03 package.[19] The 6-31G basis

(15) (a) Sasaki, D. Y.; Shnek, D. R.; Pack, D. W.; Arnold, F. H. *Angew. Chem., Int. Ed. Engl.* **1995**, *34*, 905−907. (b) Kramer, R. *Angew. Chem., Int. Ed.* **1998**, *37*, 772−773. (c) Zheng Y.; Gattás-Asfura, K. M.; Konka, V.; Leblanc, R. M. *Chem. Commun.* **2002**, 2350−2351. (d) Roy, B. C.; Chandra, B.; Hromas, D.; Mallik, S. *Org. Lett.* **2003**, *5*, 11−14. (e) Fernandez, Y. D.; Gramatges, A. P.; Amendola, V.; Foti, F.; Mangano, C.; Pallavicini, P.; Patroni, S. *Chem. Commun.* **2004**, 1650−1651. (f) Xu, Z.; Qian, X.; Cui, J. *Org. Lett.* **2005**, *7*, 3029−3032. (g) Xiang, Y.; Tong, A.; Jin, P.; Ju, Y. *Org. Lett.* **2006**, *8*, 2863−2866.

(16) (a) Barnham, K. J.; Masters, C. L.; Bush, A. L. *Nat. Rev. Drug Discovery* **2004**, *3*, 205−214. (b) Pontiki, E.; Hadjipavlou-Litina, D.; Chaviara, A. T.; Bolos, C. A. *Bioorg. Med. Chem. Lett.* **2006**, *16*, 2234−2237. (c) Moret, V.; Laras, Y.; Pietrancosta, N.; Garino, C.; Guéléver, G.; Rolland, A.; Mallet, B.; Norreel, J.-C.; Kraus, J.-L. *Bioorg. Med. Chem. Lett.* **2006**, *16*, 3298−3301.

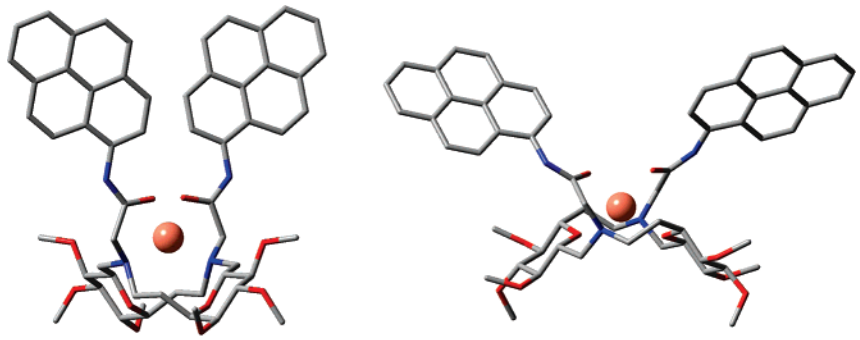

FIGURE 8. B3LYP/6-31G energy-minimized structures of the Cu^{2+}-complexed ligands **1** (left) and **2** (right) by DFT calculations. (To simplify the calculation, methyl ethers were used as hydroxy protecting groups.) The LANL2DZ (ECP) basis set was used for the Cu^{2+} cation.

sets were used except for Cu^{2+}, where LANL2DZ effective core potential (ECP) was employed. The molecular geometry optimization of both ligands without cation shows that the two pyrenyl substituents are free to adopt many accessible conformations. The absence of clear minima in the potential energy surfaces reveals that the flexibility required to form excimers is achieved in the free ligands (Supporting Information). Figure 8 displays the predicted structures corresponding to the Cu^{2+} complexes of ligands **1** and **2**. The Cu^{2+} cation is shown to be coordinated with the two carbonyl groups and the two amino groups of the sugar-aza-crown of ligand **1**. In the case of ligand **2**, two additional oxygen atoms from the sugar-aza-crown are involved into the coordination sphere, which can explain the higher stability constant of the complex. On the other hand, the conformational states of both complexes are clearly rigidified by the metal coordination with the pyrene moieties placed far apart. As a result, excimer formation is conformationally prohibited in the complexes, which illustrates the complete quenching of the excimer emission.

Conclusion

Two Cu^{2+}-selective fluoroionophores were designed and synthesized by the combination of sugar-aza-crown and pyrene chromophore. Both ligands show a 1:1 stoichiometry with high binding constants and a detection limit in the nanomolar range. The Cu^{2+}-induced fluorescence quenching can be ascribed by a PET from the excited pyrene to the complexed Cu^{2+} cation. The excimer-to-monomer ratio decreases as a function of Cu^{2+} concentration, allowing ratiometric measurements to determine accurately the equivalent point in the case of ligand **2**. Computational calculations showed that excimer formation is prohibited within the complexes because of a strong conformational rigidification of the ligands upon binding of Cu^{2+}. The successful use of pyrenyl sugar-aza-crown ethers as Cu^{2+}-selective fluoroionophores opens the way for the design of new ligands for supramolecular chemistry based on the sugar-aza-crown frameworks.

Experimental Section

Bis[*N*-(1-pyrenyl)aminocarbonylmethyl]sugar-aza-crown 1. To a solution of sugar-aza-crown **4**[9b] (20 mg, 0.027 mmol) in acetonitrile (3 mL) were added 2-chloro-*N*-pyrenylacetamide **5**[3b] (20 mg, 0.068 mmol), *t*BuNI (10 mg, 0.027 mmol), KI (22 mg, 0.14 mmol), and K_2CO_3 (15 mg, 0.109 mmol). After being stirred for one night under reflux, the mixture was concentrated, dissolved in a mixture of CH_2Cl_2/H_2O containing several drops of NaOH (1 M), and separated. The aqueous layer was extracted two times with CH_2Cl_2. The organic layer was then washed with brine, dried ($MgSO_4$), concentrated, and purified on silica gel (EtOAc/cyclohexane, 1:1) to afford the compound **1** as a pale green solid (27 mg, 80%). R_f 0.55 (EtOAc/cyclohexane, 9:1), mp 107 °C, $[\alpha]_D$ +150.4° (*c* 1, CH_2Cl_2), FTIR: 1690 cm^{-1}. ^1H NMR (250 MHz, $CDCl_3$) δ 2.08−2.42 (m, 4H, 2 × H-2), 2.98 (dd, J = 8.8, 13.4 Hz, 2H, 2 × H-6′a), 2.90−3.11 (m, 2H, 2 × H-1a), 3.17−3.53 (m, 8H, 2 × H-1b, 2 × H-4′, 2 × H-6′b, 2 × CH−Ar), 3.32 (s, 6H, 2 × CH_3(MOM)), 3.35 (s, 6H, 2 × CH_3(MOM)), 3.61 (d, J = 17.3 Hz, 2H, 2 × CH−Ar), 3.67−3.85 (m, 4H, 2 × H-2′, 2 × H-3′), 4.03−4.17 (m, 2H, 2 × H-5′), 4.26−4.39 (m, 2H, 2 × H-1′), 4.46 (d, J = 6.5 Hz, 2H, 2 × CHOMe), 4.56 (d, J = 11.4 Hz, 2H, 2 × OCH−Ph), 4.64 (d, J = 6.5 Hz, 2H, 2 × CHOMe), 4.74 (d, J = 11.1 Hz, 2H, 2 × OCH−Ph), 4.75 (d, J = 6.8 Hz, 2H, 2 × CH−OMe), 4.87 (d, J = 6.8 Hz, 2H, 2 × CH−OMe), 7.12−7.25 (m, 10H, Ph), 7.66−7.92 (m, 10H, Ar), 7.92−8.04 (m, 4H, Ar), 8.15 (d, J = 9.3 Hz, 2H, Ar), 8.63 (d, J = 8.3 Hz, 2H, Ar), 10.36 (s, 2H, 2 × NH). ^{13}C NMR (62.9 MHz, $CDCl_3$) δ 23.1 (C-2), 49.6 (C-1), 55.9 (CH_3(MOM)), 56.5 (CH_3(MOM)), 58.5 (CH_2−Ar), 60.3 (C-6′), 71.3 (C-5′), 72.5 (C-1′), 75.5 (CH_2−Ph), 78.5 (C-2′), 79.6 (C-4′), 81.6 (C-3′), 98.0, 98.6 (CH_2(MOM)); 119.5, 120.1 (Ar); 122.0, 124.4 (C_{ipso}); 124.7 (Ar), 124.9 (C_{ipso}), 125.2, 125.3, 125.9, 126.4, 127.2 (Ar); 127.7, 127.8 (Ph); 128.3 (C_{ipso}), 128.5 (Ph), 130.4, 130.5, 131.2, 138.2 (C_{ipso}); 169.5 (CO). MS (ESI-HRMS): *m/z* calcd for $C_{74}H_{81}N_4O_{14}$ $[M + H]^+$ 1249.5744, obsd 1249.5743; calcd for $C_{74}H_{80}N_4O_{14}Na$ $[M + Na]^+$ 1271.5563, obsd 1271.5558; calcd for $C_{74}H_{80}N_4O_{14}K$ $[M + K]^+$ 1287.5303, obsd 1287.5300.

Bis[*N*-(1-pyrenyl)aminocarbonylmethyl]sugar-aza-crown 2. To a solution of sugar-aza-crown **6**[9b] (50 mg, 0.081 mmol) in acetonitrile (7.5 mL) were added 2-chloro-*N*-pyrenylacetamide **5** (60 mg, 0.264 mmol), *t*BuNI (30 mg, 0.081 mmol), KI (67 mg, 0.407 mmol), and K_2CO_3 (45 mg, 0.326 mmol). After being stirred

(17) Singhal, N. K.; Ramanujam, B.; Mariappanadar, V.; Rao, C. P. *Org. Lett.* **2006**, *8*, 3525−3528.

(18) (a) Stephen, H.; Geipel, G.; Appelhans, D.; Bernhard, G.; Tabuani, D.; Komber, H.; Voit, B. *Tetrahedron Lett.* **2005**, *46*, 3209−3212. (b) Kim, S. H.; Park, S. M.; Chang, S.-K. *Org. Lett.* **2006**, *8*, 371−374.

(19) Frisch, M. J.; Trucks, G. W.; Schlegel, H. B.; Scuseria, G. E.; Robb, M. A.; Cheeseman, J. R.; Montgomery, J. A., Jr.; Vreven, T.; Kudin, K. N.; Burant, J. C.; Millam, J. M.; Iyengar, S. S.; Tomasi, J.; Barone, V.; Mennucci, B.; Cossi, M.; Scalmani, G.; Rega, N.; Petersson, G. A.; Nakatsuji, H.; Hada, M.; Ehara, M.; Toyota, K.; Fukuda, R.; Hasegawa, J.; Ishida, M.; Nakajima, T.; Honda, Y.; Kitao, O.; Nakai, H.; Klene, M.; Li, X.; Knox, J. E.; Hratchian, H. P.; Cross, J. B.; Bakken, V.; Adamo, C.; Jaramillo, J.; Gomperts, R.; Stratmann, R. E.; Yazyev, O.; Austin, A. J.; Cammi, R.; Pomelli, C.; Ochterski, J. W.; Ayala, P. Y.; Morokuma, K.; Voth, G. A.; Salvador, P.; Dannenberg, J. J.; Zakrzewski, V. G.; Dapprich, S.; Daniels, A. D.; Strain, M. C.; Farkas, O.; Malick, D. K.; Rabuck, A. D.; Raghavachari, K.; Foresman, J. B.; Ortiz, J. V.; Cui, Q.; Baboul, A. G.; Clifford, S.; Cioslowski, J.; Stefanov, B. B.; Liu, G.; Liashenko, A.; Piskorz, P.; Komaromi, I.; Martin, R. L.; Fox, D. J.; Keith, T.; Al-Laham, M. A.; Peng, C. Y.; Nanayakkara, A.; Challacombe, M.; Gill, P. M. W.; Johnson, B.; Chen, W.; Wong, M. W.; Gonzalez, C.; Pople, J. A. *Gaussian 03*, revision C.02; Gaussian, Inc.: Wallingford, CT, 2004.

for one night under reflux, the mixture was concentrated, dissolved in a mixture of CH_2Cl_2/H_2O containing several drops of NaOH (1 M), and separated. The aqueous layer was extracted two times with CH_2Cl_2. The organic layer was then washed with brine, dried ($MgSO_4$), concentrated, and purified by HPLC (CH_3CN/H_2O containing 0.1% TFA, 60:40 to 70:30 in 30 min) to afford the compound **2** as a pale green solid (27 mg, 29%). R_f 0.55 (EtOAc/cyclohexane, 9:1), mp 272 °C (dec), $[\alpha]_D$ −89.4° (*c* 0.5, CH_2Cl_2), FTIR: 1691, 1658 cm^{-1}. ^1H NMR (250 MHz, $CDCl_3$) δ 1.50−1.73 (m, 2H, 2 × H-2a), 1.95−2.13 (m, 2H, 2 × H-2b), 2.78−3.03 (m, 8H, 2 × H-1a, 2 × H-6′a, 2 × H-2′, 2 × H-4′), 3.10 (d, J = 13.9 Hz, 2H, 2 × H-6′b), 3.33 (d, J = 16.9 Hz, 2H, 2 × CH−Ar), 3.38−3.68 (m, 8H, 2 × H-1b, 2 × H-1′, 2 × H-5′, 2 × H-3′), 3.45 (s, 6H, 2 × OCH_3), 3.49 (s, 6H, 2 × OCH_3), 3.61 (d, J = 16.9 Hz, 2H, 2 × CH−Ar), 4.57 (s, 4H, 2 × CH_2−Ph), 7.14−7.29 (m, 10H, Ph), 7.75−7.87 (m, 4H, Ar), 7.94−8.06 (m, 6H, Ar), 8.11 (dd, J = 6.8, 2.5 Hz, 2H, Ar), 8.18 (d, J = 5.6 Hz, 2H, Ar), 8.22 (d, J = 6.5 Hz, 2H, Ar), 8.59 (d, J = 8.3 Hz, 2H, Ar), 9.88 (s, 2H, 2 × NH). ^{13}C NMR (62.9 MHz, $CDCl_3$) δ 28.9 (C-2), 51.3 (C-1), 56.5 (C-6′), 60.6 (CH_2−Ar), 61.1, 61.2 (OMe); 75.3 (CH_2−Ph), 71.3 (C-5′), 72.5 (C-1′), 75.5 (CH_2−Ph), 77.4, 82.1, 82.5, 83.7, 87.3, 120.7, 121.3, 123.3, 124.9, 125.0, 125.3, 125.4, 126.1, 126.6, 127.4, 127.8, 127.9, 128.5, 129.0, 130.7, 130.8, 131.4, 138.4, 170.1. MS (ESI-HRMS): *m*/*z* calcd for $C_{70}H_{73}N_4O_{10}$ $[M + H]^+$ 1129.5321, obsd 1129.5320; calcd for $C_{70}H_{72}N_4O_{10}Na$ $[M + Na]^+$ 1151.5141, obsd 1151.5138.

N-Pyrenylacetamide **3** was prepared following the literature procedure.[11]

Acknowledgment. Pr. P. Audebert and Dr. F. Miomandre are acknowledged for the electrochemical potential measurements.

Supporting Information Available: General methods, ^1H and ^{13}C NMR spectra of compounds **1** and **2**, additional fluorescence and absorption spectra, electrochemical potential measurements, and complete details of computational methods and results. This material is available free of charge via the Internet at http://pubs.acs.org.

JO070315Y